15

Optical measurements of shrinkage and temperature distribution during microwave sintering

© S.V. Egorov, A.G. Eremeev, K.I. Rybakov, A.A. Sorokin, V.V. Kholoptsev

Federal Research Center A.V. Gaponov-Grekhov Institute of Applied Physics of the Russian Academy of Sciences, Nizhny Novgorod, Russia
e-mail: rybakov@ipfran.ru

Received July 9, 2025
Revised September 18, 2025
Accepted November 21, 2025

A combined optical diagnostics method for high-temperature microwave processing of materials is described. It enables rapid acquisition of information on changes in the size and shape of an object and on the temperature distribution over its surface based on the processing of infrared digital images. The application of this method to rapid microwave reaction sintering of Ce:YAG + Al_2O_3 composite ceramic materials is discussed. The design of the developed device for extracting optical radiation from the workchamber is described, ensuring protection of the sensitive elements of the optical system from intense microwave radiation.

Keywords: high-temperature microwave processing of materials, optical dilatometry, yttrium aluminum garnet, gyrotron.

DOI: 10.61011/TP.2026.03.63171.176-25

Introduction

Microwave sintering is a promising method for materials consolidation, which is characterized by high energy efficiency, allows for a significant reduction in the duration of high-temperature processing, and results in materials with improved microstructure and properties [1].

Diagnostic methods, which are needed to implement automatic equipment control and identify optimal microwave processing regimes, are central to microwave sintering processes. As rapid sintering methods are being developed [2], the requirements as to the speed and accuracy of diagnostic methods become more stringent. The traditional method of recording densification curves, which involves heating identical samples to different temperatures, is very labor-intensive. To measure shrinkage during microwave heating processes, it was proposed to use the contact dilatometry method, where a dielectric (ceramic) rod connected to an inductive displacement sensor is brought into contact with the sample undergoing densification [3]. The disadvantage of this method is the possible distortion of measurement results associated with rod deformation due to its microwave heating.

Non-contact optical diagnostic methods are more effective under the conditions of intense microwave heating. The authors of [4] have proposed to use the optical triangulation method for non-contact dilatometry during microwave sintering. The position of a laser beam reflected from the surface of the sample undergoing densification was recorded by a position-sensitive detector. Obviously, the plane-parallel nature of the sample surfaces needs to be maintained for this method to be accurate. In addition, the detector should not be sensitive to the thermal radiation of the heated sample. Later, methods based on the observation of the samples undergoing heating with optical digital cameras and further processing of the obtained images have been proposed. For example, a 12-bit CCD camera with the maximum sensitivity in the visible light region and a long-focus lens were used for dilatometry in microwave heating processes in a 2.45 GHz multimode cavity [5]. Coupled with an optical pyrometer, this system allowed one to obtain data on temperature of the monitored object. A similar system with an 8-bit camera and mirror decoupling between the pyrometer and the camera was used in [6] for dilatometry during microwave sintering of alumina. The reconstruction of temperature distribution over the surface of a sample based on optical measurements during microwave sintering of hydroxyapatite was discussed briefly in [7].

In the present study, we develop a combined method of optical diagnostics, which allows for rapid acquisition of data on changes in the size and shape of a sample and on the temperature distribution over its surface through processing of infrared digital images. The proposed method is suitable for non-contact measurements of sample shrinkage during sintering and temperature differences on the sample surface; however, it requires calibration of the absolute temperature value, which is performed in the described implementation via thermocouple measurements. The design of a device for optical radiation output from the workchamber, which protects sensitive elements of the optical system from intense microwave radiation, is detailed. The application of this method in rapid sintering processes of composite ceramic materials under microwave heating is discussed.

1. Experimental methods

Sintering experiments were carried out using a specialized gyrotron system for high-temperature microwave processing

of materials [8]. Microwave radiation generated by a gyrotron with a maximum power of approximately 6 kW operating at a frequency of 24 GHz was fed into the workchamber with a volume close to 0.1 m^3, which presents an oversized multimode cavity. A movable mode stirrer was used to make the electromagnetic field distribution in the workchamber more uniform.

The samples prepared for experiments had the form of pellets with a diameter of 10 mm and an approximate thickness of 2.5 mm obtained by pressing a mixture of nanosized powders of Al_2O_3 and Y_2O_3 doped with CeO_2. The mass ratio between the mixture components was chosen so as to obtain a composition of 70 mass % Ce:YAG (0.2 at.% Ce^{3+}) + 30 mass % Al_2O_3 as a result of reaction sintering [9]. The relative density of compacted samples was close to 30 % of the theoretical value.

The sample undergoing processing was positioned in the workchamber of the gyrotron system in a heat-insulating container 150 × 50 × 25 mm in size with a through channel with a diameter of 11 mm drilled in the horizontal plane. The AL-30 material (Zircar Ceramics, United States) based on highly porous alumina, which is characterized by low thermal conductivity and a low coefficient of absorption of electromagnetic radiation, was used as heat insulation. For additional temperature equalization, the sample was placed inside a sintered alumina ring embedded into the heat-insulating container. The sample temperature was measured with a platinum-rhodium (type B) thermocouple. The thermocouple head was positioned in a hole with an approximate diameter of 1.5 mm drilled to the center of the sample. The accuracy of thermocouple temperature measurements, determined in separate calibration experiments on microwave heating of samples of metals and inorganic compounds to known melting points, was no worse than ±0.7 %. The temperature readings obtained from the thermocouple were used throughout the entire process for automatic power control of the gyrotron microwave source in accordance with the specified temperature-time schedule and for calibration of optical temperature measurements, as described below. The sample under investigation was positioned vertically in the middle part of the channel, which allowed for its visual inspection *in situ* using the optical dilatometry system.

In the experiments discussed below, heating was performed at a constant rate of 10 °C/min to a temperature of 1650 °C. The process included an intermediate 10-min hold at a temperature of 600 °C that was needed to remove the adsorbed water. The heating rate was chosen based on the condition of obtaining integral sintered Ce:YAG + Al_2O_3 samples within the minimum process time. Depending on the material being studied, different heating rates, which went as high as several hundred °C/min [2] at the high-temperature stage, were used for microwave sintering. An increase in microwave heating rate allows for a significant reduction in the duration of the sintering process, but requires an increased density of the volumetrically deposited power, which translates into a less uniform temperature distribution within the sample and imposes stricter requirements as to the stability of the heating process.

The key elements of the optical dilatometry system are a digital monochrome camera with an increased sensitivity in the near infrared range and an optical lens that allows for high-resolution recording of small spatial changes in the sample during its densification. The NET 3iCube monochrome camera with a 1/2 inch CMOS sensor (NET GmbH, Germany) used in the system has a horizontal and vertical resolution of 1280 × 1024 pixels, a maximum frame rate of 60 fps, and a maximum data transfer rate of 5 Gbit/s. The VSZ-0745 lens with a VSZ-0.3X front converter (VS Technology, Japan) has the capacity to focus on an object 10−15 mm in size at a distance up to 337 mm, which corresponds to the configuration of the microwave heating experiments. This optical system allows one to expand the image of the sample with an approximate diameter of 10 mm to fill the entire frame and measure small shrinkage values in real time. The Stream Pix 7 software (Norpix, Canada) was used to adjust the brightness of images from the camera automatically, transmit a sequence of images to a computer and record it, and display them on a monitor.

Another important element of the optical system is the window for optical radiation output from the workchamber of the gyrotron system. It is designed as a sandwich of two quartz glasses with distilled water circulating between them. The workchamber/window assembly is vacuum-tight and protects the optical system elements reliably from intense microwave radiation. An infrared filter (IKS3 or IKS5) can be integrated into the optical radiation output system. Coaxial fiber illumination was used in the optical system to measure the dimensions of a cold sample before and after microwave heating.

A schematic diagram of the workchamber with the heat-insulating container and the optical system is shown in Fig. 1.

Processing the data obtained by the system allows one to monitor the shrinkage of samples throughout the entire microwave sintering process, evaluate temperature non-uniformity, and observe the development of thermal instabilities. To determine the shrinkage, the shape of the sample in infrared images was approximated by an ellipse, and the geometric mean of its semi-axes was taken as the equivalent diameter.

The temperature distribution over the sample surface was determined based on the brightness data for elements of images obtained by the infrared camera. According to Planck's formula, the spectral density of radiation emitted by a heated body is

$$I_\lambda = \varepsilon_\lambda I_\lambda^0 = \varepsilon_\lambda \frac{C_1}{\lambda^5[\exp(\frac{C_2}{\lambda T}) - 1]},$$

where ε_λ is the spectral emissivity of the body; I_λ^0 is the blackbody spectral density; $C_1 = 3.7405 \cdot 10^{-16}$ W·m^2 and $C_2 = 1.43879 \cdot 10^{-2}$ m·K are the first and second radiation

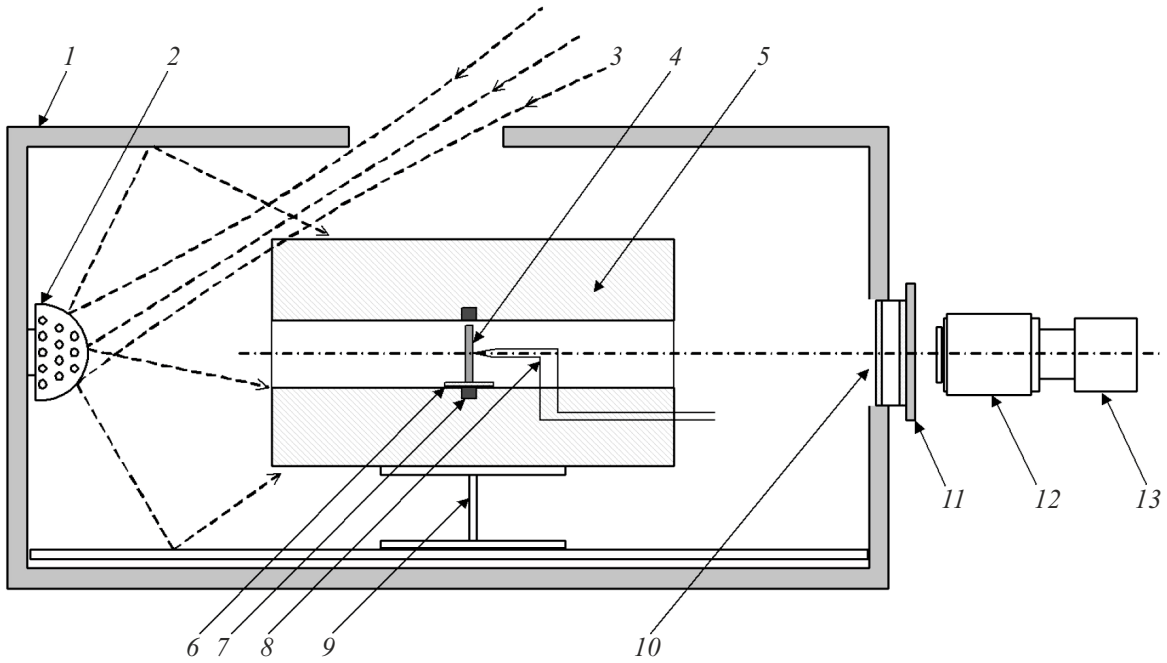


Figure 1. Diagram of the experimental setup for rapid microwave sintering with an optical diagnostic system: *1* — workchamber, *2* — mode stirrer, *3* — microwave beam from the gyrotron, *4* — sample, *5* — heat-insulating container, *6* — sapphire holder, *7* — sintered alumina ring, *8* — thermocouple, *9* — adjustable stage, *10* — optical radiation output window, *11* — infrared filter, *12* — lens, and *13* — infrared camera.

constants, respectively; λ is the radiation wavelength; and T is absolute temperature.

Since radiation is detected by an optical camera with an infrared (IR) filter normally positioned in front of it, the image brightness is determined not just by the intensity of radiation of the examined body, but also by the spectral properties of the camera and the IR filter used. The image brightness B_{image} is calculated as

$$B_{image} = \int_0^\infty \varepsilon_\lambda I_\lambda^0 S_\lambda T_f d\lambda,$$

where S_λ is the spectral sensitivity of the camera and T_f is the filter transmittance. Assuming that ε_λ varies little within the camera and filter pass bands, one may write

$$B_{image} = \varepsilon \int_0^\infty I_\lambda^0 S_\lambda T_f d\lambda = \varepsilon \Phi(T),$$

where

$$\Phi(T) = \int_0^\infty I_\lambda^0 S_\lambda T_f d\lambda.$$

The function $\Phi(T)$ for the camera without and with IKS3 and IKS5 filters is plotted in Fig. 2.

During the experiment, the camera is operated in the mode of automatic maintenance of a constant level of average image brightness, which is achieved by varying the

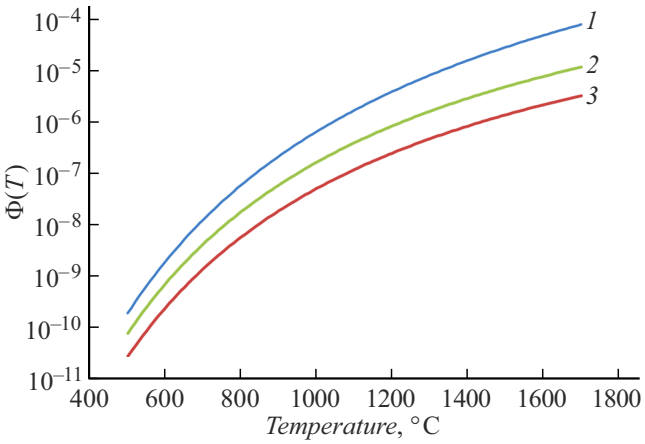


Figure 2. Function $\Phi(T)$ for: *1* — camera without filters, *2* — camera with an IKS5 filter, and *3* — camera with an IKS3 filter.

exposure time of each frame. Therefore, the absolute value of brightness is not indicative of the sample temperature. To determine the temperature, the image brightness was compared to temperature readings of the thermocouple located at the center of the sample. Matching the values of image brightness B_{th} at points close to the thermocouple head to the temperature T_{meas} measured by the thermocouple, one can determine the coefficient c_b of proportionality between the image brightness and the values of function $\Phi(T)$:

$$c_b = \Phi(T_{meas})/B_{th}.$$

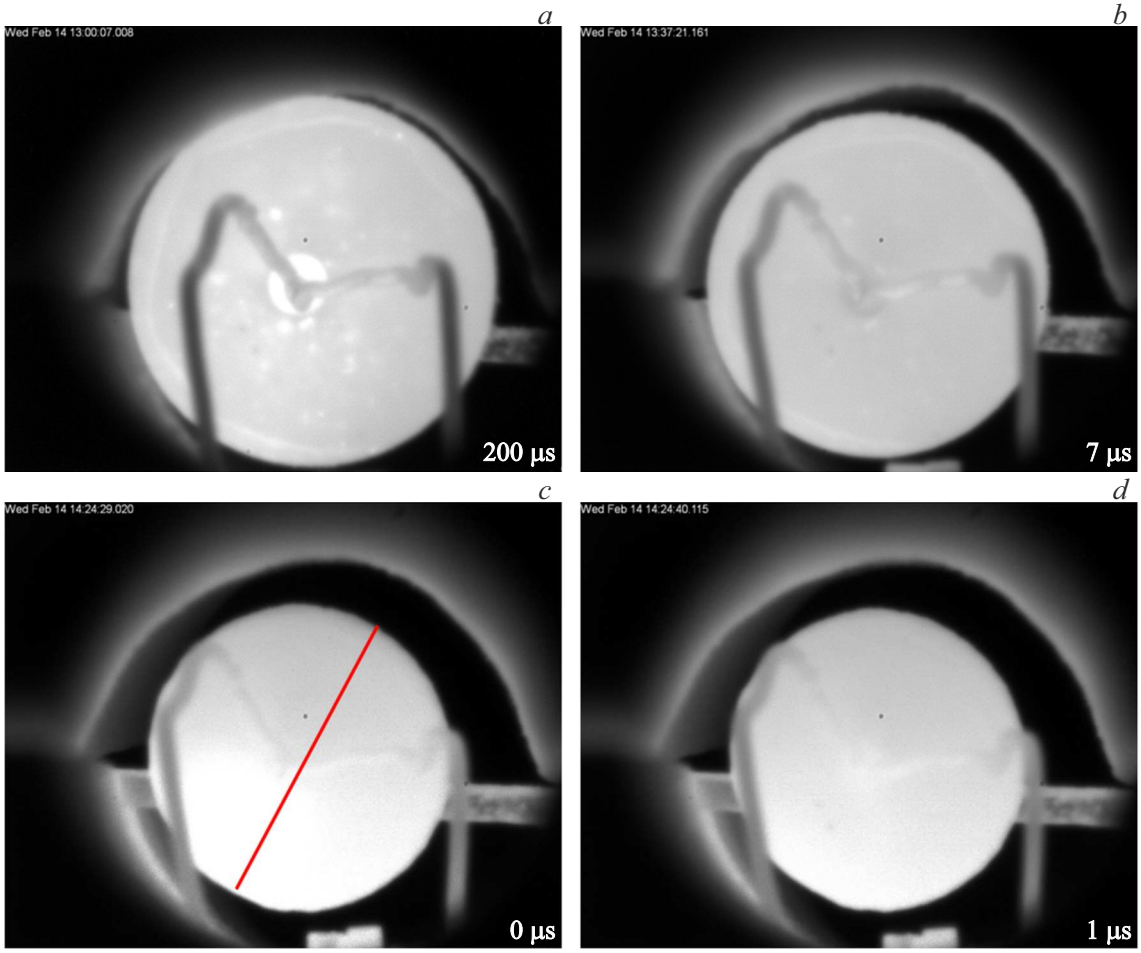


Figure 3. Infrared images of a Ce:YAG + Al_2O_3 sample in the process of microwave heating at a rate of 10 °C/min obtained at the following temperatures of the center of the sample: *a* — 800 °C, *b* — 1150 °C, *c* — 1650 °C, and *d* — 1625 °C (cooling stage).

Using this coefficient, the brightness of each image point can be recalculated into values of Φ, and then, using the inverse function $T(\Phi)$, the temperature of each point of the sample surface can be determined.

Samples obtained at different microwave heating temperatures were subjected to X-ray diffraction (XRD) analysis with an Ultima IV X-ray diffractometer (Rigaku, Japan) in order to establish a correlation between temperature, density (shrinkage), and phase composition.

2. Results and discussion

The nature of microwave heating of samples is illustrated by images from the infrared camera of the optical dilatometry system presented in Fig. 3. The characteristic pattern of volumetric heating is observed starting from the moment when the temperature at the center of the sample reaches approximately 750 °C: the inner region of the sample (visible in the thermocouple hole) is brighter (i.e., hotter) than the surface (Fig. 3, *a*). Heating becomes noticeably non-uniform (small brighter areas on the surface) within the 800 °C–860 °C temperature range. This may be attributed to phase transformations in the material and differences in absorption of microwave radiation in regions corresponding to different crystalline phases. This is the first stage of sample shrinkage (see below). The volumetric heating pattern vanishes at temperatures upward of approximately 1150 °C, which is apparently attributable to an increase in absorption in the sintered alumina ring surrounding the sample. The brightness of the entire sample is approximately uniform in the corresponding image (Fig. 3, *b*). At the final stage of heating (at a temperature of approximately 1650 °C), heating non-uniformity is detected in the form of a bright spot, which is shifted in the particular experimental run to the left and downward from the center of the sample (along the line in Fig. 3, *c*). This is accompanied by intense shrinkage. After the maximum temperature is reached and the microwave radiation source is turned off, the sample shrinkage ceases, and the non-uniformity of the temperature distribution diminishes gradually (Fig. 3, *d*).

The plots of linear shrinkage and the automatically controlled power during microwave heating in Fig. 4 illustrate the results of studies of shrinkage of Ce:YAG + Al_2O_3 sam-

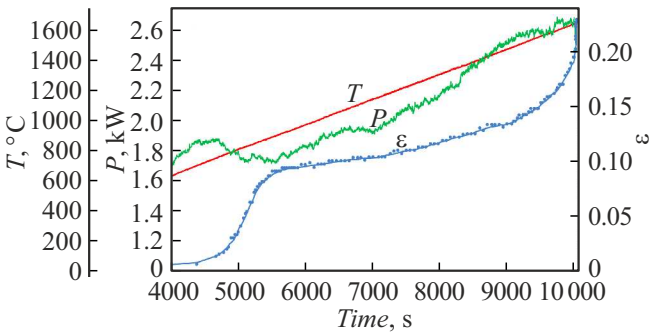


Figure 4. Temperature (T), automatically controlled microwave power (P), and relative linear shrinkage (ε) recorded at the high-temperature stage of microwave heating of a Ce:YAG + Al_2O_3 sample at a rate of 10 °C/min.

ples during microwave sintering with the optical dilatometry system.

It follows from Fig. 4 that the shrinkage rate has two maxima. The first maximum is observed at a temperature of approximately 800 °C and corresponds to a decline in the microwave power. Having passed this maximum, the shrinkage rate drops by more than an order of magnitude. With a further increase in temperature, a noticeable increase in shrinkage rate is observed again only at 1500 °C.

The results of XRD studies revealed [9] that the first maximum of shrinkage rate corresponds to the transformation of alumina from the initial low-temperature metastable η phase into the stable α phase, which has a higher density. An increase in density results in enhanced microwave absorption in the material, and the microwave power, which is adjusted automatically to maintain a given heating rate, is reduced. A similar acceleration of shrinkage within the temperature range corresponding to this phase transformation was observed during microwave sintering of Al_2O_3 + YSZ ceramic composites (YSZ is yttria-stabilized zirconia) [10].

The second maximum of the shrinkage rate is found at the final stage of sintering. Since the temperature distribution is non-uniform at this point (see below), shrinkage does not proceed completely uniformly throughout the sample. It can be seen from Fig. 3, *c* that the observed shape of the sample differs somewhat from a circle, which is attributable to faster shrinkage in the region of maximum temperature. However, shrinkage is equalized later, and the sintered samples are fairly close in shape to a circular cylinder.

The results of the study of temperature distribution over the surface of the sample are presented in Figs. 5, 6. Figure 5 shows the radial temperature distributions averaged over the angular coordinate, corresponding to different instants of time during the process of microwave heating. It is easy to see that microwave heating of the material does, on average, remain quite uniform throughout the entire high-temperature sintering stage. A slight drop in temperature along the edge of the sample is attributable to heat loss from the side surface adjacent to the heat-insulating assembly.

However, the temperature distribution along the angular coordinate is not completely uniform at the later stages of microwave sintering. Figure 6 shows the temperature distribution along the diameter of the sample indicated by the line in Fig. 3, *c*. It follows from the presented data that the approximate magnitude of temperature variation along this diameter is 80 °C within the range of sample center temperatures of 1550 °C–1650 °C. Reliable data on the maximum temperature are lacking at higher temperatures, since the automatic exposure control system, which maintains a constant average brightness of the frame, leaves the brightest region overexposed (in Fig. 6, these regions are denoted by straight horizontal segments corresponding to the maximum brightness levels; they were excluded from the averaging procedure when the distributions shown in Fig. 5 were plotted).

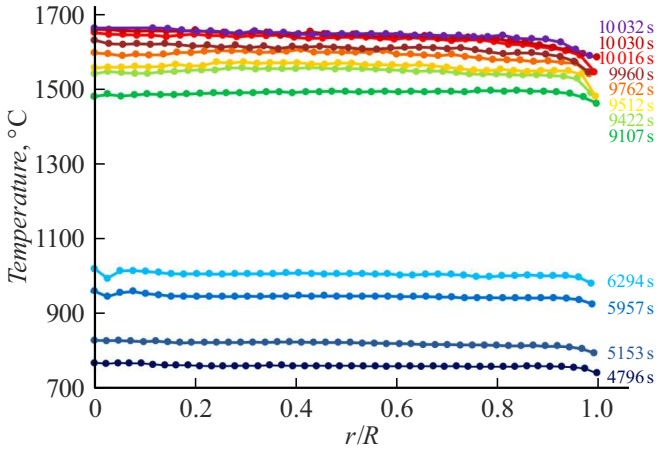


Figure 5. Radial temperature distributions for a Ce:YAG + Al_2O_3 sample averaged over the angular coordinate and corresponding to different instants of time during the process of microwave heating at a rate of 10 °C/min.

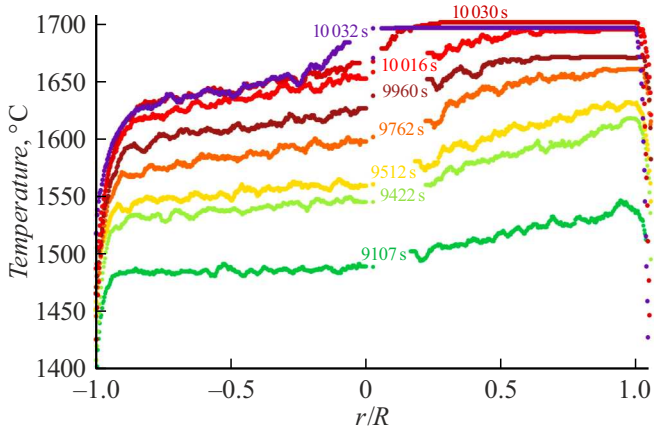


Figure 6. Temperature distributions along the diameter of the Ce:YAG + Al_2O_3 sample indicated by the line in Fig. 3, *c* corresponding to different instants of time during the process of microwave heating at a rate of 10 °C/min. The curves have a gap in the region where the thermocouple is located.

The non-uniformity of temperature distribution during microwave heating may be attributed to various factors: volumetric heat release, non-uniform spatial distribution of microwave electromagnetic field intensity, non-uniform heat removal due to imperfect centering of the sample in the heat-insulating assembly, etc. It is known that, under certain relationships between the density of the volumetrically released thermal power, the temperature dependence of the microwave absorption coefficient in the material undergoing heating and the conditions of heat removal during microwave heating, thermal instability may occur.

The specific power of volumetric heat release during microwave heating of a Ce:YAG + 30 mass % Al_2O_3 sample was estimated from the rate of its cooling with the microwave source switched off. At the moment when the sample center temperature was 1625 °C (11 s after switching off the microwave source; Fig. 3, *d*), the cooling rate due to heat loss was 10.4 °C/s. Since the power P released in the sample during microwave heating must compensate for heat losses, it can easily be estimated as $P = c_p m|dT/dt|$. To calculate specific heat capacity c_p of the 70 mass % YAG + 30 mass % Al_2O_3 composition within the 1400 °C–1700 °C temperature range, we used the data on specific heat capacity of alumina and yttrium-aluminum garnet from [12] and [13], respectively. The obtained estimate of the power P was close to 3.0 W. Since the approximate volume of samples after sintering is 0.1 cm^3, the specific power of volumetric heat release during microwave heating at the high-temperature stage of the process is approximately 30 W/cm^3 (if we assume that heat losses at the same temperatures at the heating and cooling stages are equal).

Combined with heat removal from the sample surface, volumetric heat release necessarily generates a non-uniform temperature distribution within the sample. The problem under study is characterized by two different scales of non-uniformity: a larger one along the radius of the sample and a smaller one along its thickness. Estimates based on reconstructed angle-averaged temperature distributions along the radius yield a radial temperature gradient dT/dr of approximately 37 °C/cm. The integral heat flow rates along the radius and thickness were estimated as $P_r = \lambda\pi dh \cdot dT/dr$ and $P_t = P - P_r = 2\lambda\pi d^2\Delta T_t/h$, respectively ($\lambda$ is the thermal conductivity coefficient of the material, d and h are the diameter and height of the sample, and ΔT_t is the temperature difference across the thickness between the midplane and the surface of the sample). It was found that the radial heat flow carries away approximately 25 % of thermal power released in the sample, while the flow along the thickness carries away the other 75 %. The temperature difference ΔT_t across the thickness of the sample does not exceed 1.1 °C. For these estimates, the value of thermal conductivity λ of the composite material was calculated using the effective medium approximation method and the data for alumina and yttrium-aluminum garnet from [12] and [14], respectively; the difference in thermal conductivity between partially sintered and fully dense materials was taken into account in accordance with the results reported in [15].

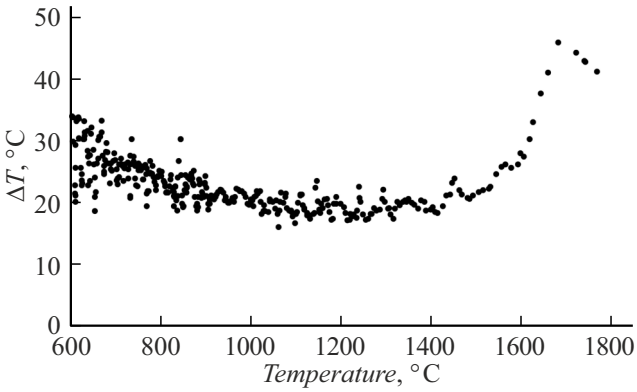


Figure 7. Temperature difference between the surface of the Ce:YAG + Al_2O_3 sample and the cylindrical surface of the through channel in the heat-insulating assembly facing it as a function of temperature at the center of the sample.

It should be noted that one of the factors stabilizing the microwave heating process is the incomplete microwave transparency of the material used in the heat-insulating assembly. If this material absorbs microwave radiation to a certain extent, the power of heat release inside the sample required to heat it at a given rate is reduced. Partial heating of insulation constrains the heat flow from the sample and stabilizes its temperature.

The temperature difference between the sample surface and the cylindrical surface of the through channel in the heat-insulating assembly facing it was estimated based on the data on the sample cooling rate at the cooling stage, which were used to evaluate heat loss as a function of temperature. The temperature of the heat-insulating material was estimated under the assumption that losses were radiative in nature. The evaluation results are presented in Fig. 7. It is clear that the temperature difference between the sample and the heat insulation remains at the level of 20 °C within the greater part of the temperature range of microwave sintering and exceeds 40 °C only at the short final stage.

Conclusion

A combined optical method of infrared imaging, which allows for simultaneous measurements of shrinkage of samples and temperature distribution in them in the process of rapid microwave sintering, was developed. A high-speed monochrome camera with a CMOS sensor and a precision optical system were used to obtain infrared images.

The sample shrinkage was determined by approximating the observed shape of the sintered sample with an ellipse, measuring its semi-axes, and using the equivalent circle

diameter as a measure of the current linear size of the sample.

Temperature distributions were determined based on the brightness of digital image elements (with the spectral characteristics of the used camera and optical filters taken into account). The obtained temperature values were calibrated against thermocouple measurement data. The experimentally determined characteristics of the obtained temperature distributions were compared with estimates of temperature non-uniformity in the materials undergoing heating. The proposed approach allows one to record and evaluate the degree of uniformity of temperature distribution in heated samples and to examine the development of thermal instabilities that arise under certain conditions in microwave heating processes.

In situ measurements of sample shrinkage and temperature profile dynamics combined with automatic control of microwave power provided an opportunity to study in detail the features of the process of synthesis of Ce:YAG + Al_2O_3 samples in rapid reaction sintering processes under heating by intense microwave radiation. It was found that the sample shrinkage process involves several stages: a linear shrinkage of approximately 9 % is achieved relatively fast at the first stage within the temperature range of 700 °C–900 °C, which is attributable to phase transformations in alumina. The shrinkage then slows down, but accelerates again within the temperature range of 1500 °C–1650 °C, ultimately reaching a level of approximately 23 %. At the final stage of microwave sintering of Ce:YAG + Al_2O_3 samples at a heating rate of 10 °C/min, the temperature difference along the sample diameter reaches 80 °C, while the estimated power density of volumetric heat release is close to 30 W/cm^3.

Acknowledgments

The authors wish to thank S.S. Balabanov, T.O. Evstropov, and E.Ye. Rostokina for preparing the samples used in the present study.

Funding

This study was supported by the Russian Science Foundation, grant № 23-19-00363, https://rscf.ru/project/23-19-00363/

Conflict of interest

The authors declare that they have no conflict of interest.

References

[1] Yu.V. Bykov, K.I. Rybakov, V.E. Semenov. J. Phys. D: Appl. Phys., **34**, R55 (2001). DOI: 10.1088/0022-3727/34/13/201
[2] Yu.V. Bykov, S.V. Egorov, A.G. Eremeev, I.V. Plotnikov, K.I. Rybakov, A.A. Sorokin, V.V. Kholoptsev. Tech. Phys., **63** (3), 391 (2018). DOI: 10.1134/S1063784218030052
[3] G. Link, M. Thumm. In: *Microwave and Radio Frequency Applications* (Proceedings of the Third World Congress on Microwave and Radio Frequency Applications), ed. by D.C. Folz, J.H. Booske, D.E. Clark, J.F. Gerling. (Westerville: The American Ceramic Society, 2004), p. 301.
[4] S. Marinel, E. Savary. J. Mater. Process. Technol., **209**, 4784 (2009). DOI: 10.1016/j.jmatprotec.2008.12.005
[5] D. Zymełka, S. Saunier, J. Molimard, D. Goeuriot. Adv. Eng. Mater., **13** (9), 901 (2011). DOI: 10.1002/adem.201000354
[6] J. Croquesel, D. Bouvard, J.-M. Chaix, C.P. Carry, S. Saunier. Mater. Des., **88**, 98 (2015). DOI: 10.1016/j.matdes.2015.08.122
[7] S.V. Egorov, A.G. Eremeev, V.V. Kholoptsev, I.V. Plotnikov, K.I. Rybakov, A.A. Sorokin. Mater. Today: Proc., **25**, 349 (2020). DOI: 10.1016/j.matpr.2019.12.081
[8] Yu.V. Bykov, A.G. Eremeev, M.Yu. Glyavin, G.G. Denisov, G.I. Kalynova, E.A. Kopelovich, A.G. Luchinin, I.V. Plotnikov, M.D. Proyavin, M.M. Troitskiy, V.V. Kholoptsev. Radiophys. Quant. Electron., **61** (10), 752 (2019). DOI: 10.1007/s11141-019-09933-6
[9] S.V. Egorov, A.G. Eremeev, K.I. Rybakov, A.A. Sorokin, V.V. Kholoptsev, S.S. Balabanov, T.O. Evstropov. Peculiarities of phase transformations during microwave reactive sintering of Ce:YAG–Al_2O_3 composites // Radiophys. Quant. Electron. **67** (11–12), 848 (2025). DOI: 10.1007/s11141-025-10423-1
[10] S.V. Egorov, A.G. Eremeev, V.V. Kholoptsev, I.V. Plotnikov, K.I. Rybakov, A.A. Sorokin, S.S. Balabanov, E.Ye. Rostokina. J. Eur. Ceram. Soc., **45**, 117006 (2025). DOI: 10.1016/j.jeurceramsoc.2024.117006
[11] V.E. Semenov, N.A. Zharova. In: *Advances in Microwave and Radio Frequency Processing* (Proc. 8th International Conference on Microwave and High-Frequency Heating) ed. by M. Willert-Porada (Springer, Berlin, 2006), p. 482.
[12] *Fiziko-khimicheskie svoistva okislov*, Ed. by G.V. Samsonov, The Oxide Handbook, Springer US, New York, 1973.
[13] S. Sagi, S. Hayun. J. Chem. Thermodynamics., **93**, 123 (2016). DOI: 10.1016/j.jct.2015.09.035
[14] J. Hostaša, J. Matějíček, B. Nait-Ali, D.S. Smith, W. Pabst, L. Esposito. J. American Ceramic Society, **97** (8), 2602 (2014). DOI: 10.1111/jace.13015
[15] D.S. Smith, A. Alzina, J. Bourret, B. Nait-Ali, F. Pennec, N. Tessier-Doyen. J. Mater. Res., **28**, 2260 (2013). DOI: 10.1557/jmr.2013.179

Translated by D.Safin